M&C 2017 - International Conference on Mathematics & Computational Methods Applied to Nuclear Science & Engineering, Jeju, Korea, April 16-20, 2017, on USB (2017)

Application of Weight Window Technique in Monte Carlo Calculation for Beam Design of Boron Neutron Capture Therapy

Wei-Lun Huang, Po-Lin Liao, Zhen-Fan You, Yen-Wan Hsueh Liu

Institute of Nuclear Engineering and Science, National Tsing Hua University, Hsinchu City, Taiwan, 30013

drift51877@gmail.com

Abstract - *Boron neutron capture therapy (BNCT) is an advanced cancer therapy which combines the advantage of targeted therapy and heavy particle therapy. One of the keys to the success of BNCT is a high quality epithermal neutron beam. The beam quality at the beam exit can be examined by in-phantom calculation. However, it was found to be very difficult to obtain in-phantom dose results of acceptable statistical errors within reasonable computing time. Variance reduction technique such as weight window is required. In this study, weight window technique was adopted in the MCNP calculation, including stage 1, generation of the spatial/energy dependent weight window, and stage 2, using the generated weight window for in-phantom dose calculation. The proper way to use weight window technique was analyzed. The suggestions for in weight window generation from the results include: (1) aligning mesh boundaries with material boundaries, (2) using equal lethargy for energy group structure, and (3) using number of particles that results in relative error <6% at the problem bin. By doing so, the in-phantom dose rate at depth <12 cm can be obtained with statistical error ~1% within 2hrs using 48 threads of PC-cluster.*

I. INTRODUCTION

Boron neutron capture therapy (BNCT) is an advanced cancer therapy which combines the advantage of targeted therapy and heavy particle therapy. One of the keys to the success of BNCT is a high quality epithermal neutron beam, which for a long time can only be achieved through the use of neutrons originated from nuclear research reactors. Nowadays, due to the improvement of accelerator technology, it becomes possible to install an accelerator in the hospital for BNCT purpose.

One of the feasible ways is to use a 30MeV/1mA proton beam bombarding on a beryllium target to produce high energy neutrons. After passing through properly designed beam shaping assembly (BSA), epithermal neutron beam of good quality and adequate intensity for BNCT can be achieved. The energy boundaries between thermal, epithermal and fast neutrons are 1eV and 10 keV.

The Monte Carlo code MCNPX [1] and ENDF/B-VII library was used to perform the neutron transport through the BSA. The beam quality at the exit can be examined in two ways, in-air and in-phantom. For in-phantom calculation, it was found to be very difficult to obtain results of acceptable statistical errors within reasonable computing time. Variance reduction technique such as weight window is required.

In this study, weight window technique was adopted in the MCNP calculation, including stage 1, generation of the spatial/energy dependent weight window, and stage 2, using the generated weight window for in-phantom dose calculation. The proper way to use weight window technique is analyzed, including (1) selection of energy group structure, (2) number of particle history for stage 1 weight window generation (WWG), and (3) spatial partitioning for mesh-based weight window generation.

II. MATERIALS AND METHODS

1. Simulation Model

The BSA used in this study was composed of layers of spectrum shifting material, iron, Fluental and MgF_2, followed by a layer of bismuth, and a collimator of conical shape made of bismuth (Fig. 1). Surrounding the filter were lead and concrete. Surrounding the collimator were polyethylene (PE) and lead. The BSA was 100cm thick and 160cm in diameter. An 18×18×20 cm cubic phantom was located at 10 cm away from the collimator exit and a 12×12×0.55 cm cubic beryllium target was located at the proton beam entrance.

The neutron source generated by Be(p, n) reaction was simulated as a point source at the target location. The phantom was composed of brain tissue with composition based on ICRU report 46 [2]. In the phantom dose calculation, MIT-Casewell [3] dose conversion was used. RBE for neutron was 3.2, for photon was 1[4].

MCNPX 2.6.0 together with ENDF/B-VII.0 library was used. Reference case was the case in which the in-phantom dose was calculated without using weight window technique. Number of particle history used was 4×10^8. The tally bin was along the centerline, with size 2×2 cm^2.

While generating weight window, the problem bin was set at the 10~12 cm depth in phantom, a $2\times2\times2cm^3$ cubic. F6 tally for both neutron and photon energy deposition was used.

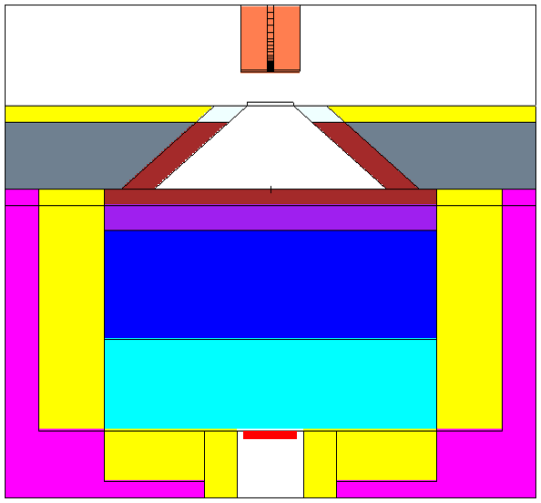

Fig. 1. Problem geometry including a beam shaping assembly, a phantom located at 10 cm away from the BSA beam exit. The beryllium target is located at the proton beam entrance.

2. Figure-of-Merit (FOM)

Figure-of-merit (FOM) is used to compare the efficiency of the calculation for accelerating the Monte Carlo calculation through weight window technique. It is defined as

$$FOM = \frac{1}{R_{\bar{x}}^2 T} \quad (1)$$

where $R_{\bar{x}}$ is the estimated relative error, and T is the computing time in minutes [5]. In this study, T is the total computing time of stage 1 and stage 2, and $R_{\bar{x}}$ is the relative error of stage 2 tally.

3. Energy Structure Selection for Mesh-Based Weight Window Generation

The first choice facing while using weight window technique in Monte Carlo calculation is the energy structure selection for mesh-based weight window generation.

The energy spectrum of neutron source produced when a 30MeV proton beam bombarding with a beryllium target is shown in Fig. 2. They are mostly fast neutrons, ranging from 4 MeV to 28.7MeV. After passing through a beam shaping assembly (BSA) specially designed for BNCT purpose, the neutrons are mostly epithermal neutrons (1eV to 10keV), as show in Fig. 3. These epithermal neutrons will be quickly slowing down to thermal neutrons when entering into brain phantom.

In MCNPX, the maximum number of energy groups for mesh-based weight window generation is 15. The effect of energy boundaries on the efficiency of the weight window technique was investigated.

Four methods were used for selecting the energy boundaries for weight window generation (Table I):

(1) Equal lethargy (Case 2a and 2b);
(2) Equal neutron source population from beryllium target (Case 2c and 2d);
(3) Equal lethargy for E< 10 keV and 10keV<E<1MeV, equal neutron source population from beryllium target for E>10keV (Case 2e and 2f);
(4) Equal neutron population based on neutron current at beam exit for E<10keV,
equal neutron population based on neutron source population from beryllium target for E>1MeV,
equal lethargy for 10keV<E<1MeV, (Case 2g).

Detailed energy boundaries and number of group in different energy range for each case was show in Table II.

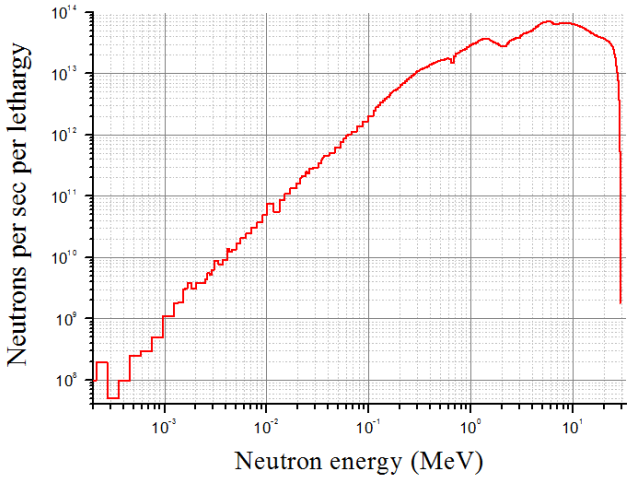

Fig. 2. Energy spectrum of neutrons produced by 30MeV proton beam bombarding with beryllium target.

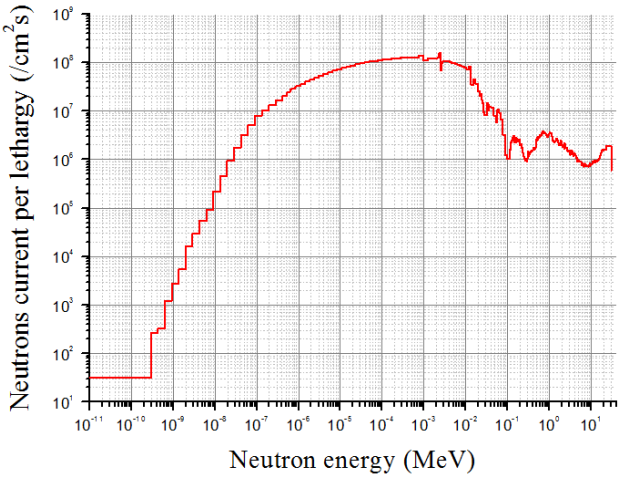

Fig. 3. Energy spectrum of neutron current at BSA exit.

Table I. Energy Structure Selection for Mesh-Based Weight Window Generation

	Method	No. of Neutron Group		
		<10keV	10keV ~ 1MeV	> 1MeV
Case 2a	Equal lethargy	15 (1eV to 30MeV)[a]		
Case 2b		15 (10eV to 30MeV)[a]		
Case 2c	Equal neutron source population	15		
Case 2d		1	14[d]	
Case 2e	Hybrid I	8[b,a]	7[d]	
Case 2f		8[b,a]	2[c]	5[d]
Case 2g	Hybrid II	8[e]	2[c]	5[d]

[a] Last group energy was extended to include thermal energy
[b] Equal lethargy (1 eV to 10 keV).
[c] Equal lethargy (10keV to 1MeV)
[d] Equal neutron population based on neutron source from beryllium target.
[e] Equal neutron population based on neutron current at beam exit .

Table II. Energy Group Upper Boundary (in MeV) for Mesh-Based Weight Window Generation

No.	Case 2a	Case 2b	Case 2c	Case 2d	Case 2e	Case 2f	Case 2g
15	3.15×10^{-6}	2.70×10^{-5}	0.42	1×10^{-2}	3.16×10^{-6}	3.16×10^{-6}	4.06×10^{-6}
14	9.93×10^{-6}	7.30×10^{-5}	0.82	0.44	1.00×10^{-5}	1.00×10^{-5}	2.04×10^{-5}
13	3.13×10^{-5}	1.97×10^{-4}	1.22	0.87	3.16×10^{-5}	3.16×10^{-5}	6.90×10^{-5}
12	9.86×10^{-5}	5.34×10^{-4}	1.73	1.31	1.00×10^{-4}	1.00×10^{-4}	1.99×10^{-4}
11	3.11×10^{-4}	1.44×10^{-3}	2.58	1.96	3.16×10^{-4}	3.16×10^{-4}	5.33×10^{-4}
10	9.79×10^{-4}	3.90×10^{-3}	3.45	2.88	1.00×10^{-3}	1.00×10^{-3}	1.46×10^{-3}
9	3.09×10^{-3}	1.05×10^{-2}	4.35	3.85	3.16×10^{-3}	3.16×10^{-3}	4.50×10^{-3}
8	9.72×10^{-3}	2.85×10^{-2}	5.24	4.89	1.00×10^{-2}	1.00×10^{-2}	1.00×10^{-2}
7	3.06×10^{-2}	7.70×10^{-2}	6.24	5.77	0.87	0.10	0.10
6	9.65×10^{-2}	2.08×10^{-1}	7.54	7.05	1.95	1.00	1.00
5	3.04×10^{-1}	5.62×10^{-1}	9.06	8.51	3.83	1.22	1.22
4	9.59×10^{-1}	1.52	11.00	10.65	5.76	3.44	3.44
3	3.02	4.11	13.74	13.35	8.52	6.21	6.21
2	9.52	11.10	18.22	17.80	13.25	10.81	10.81
1	30.00	30.00	30.00	30.00	30.00	30.00	30.00

4. Number of Particle History for Stage 1 Mesh-Based Weight Window Generation

The number of particle history used in stage 1 weight window generation will affect not only the computing time of stage 1 but also the weight window quality, which in turn will affect the computing time of stage 2 calculation and the relative error of the tally bin.

Table III shows four different number of particle histories used in stage 1. The number of particle simulated in stage 2 was 4×10^{8}. The same energy group boundary of weight window as Case 2a was used.

Table III. Number of Particle History Used in Stage 1 Weight Window Generation

	No. of Particle History in Stage 1
Case 2a	4×10^{8}
Case 3a	4×10^{7}
Case 3b	1×10^{8}
Case 3c	2×10^{8}

5. Choice of Mesh Partitioning for Mesh-Based Weight Window Generation

Use of mesh-based weight window reduces the demand of subdividing geometries for importance function [1]. Two different ways of spatial partitioning for mesh-based weight window generation were tested. Mesh 1 is to match the weight window mesh boundaries to the material boundaries with additional two partitioning in the radial direction in the BSA region, as shown in Fig. 4. Mesh 2 is to add more mesh boundaries in axial direction, mainly in each BSA layer, as shown in Fig. 5. Table IV shows the corresponding case number using mesh1 and mesh 2.

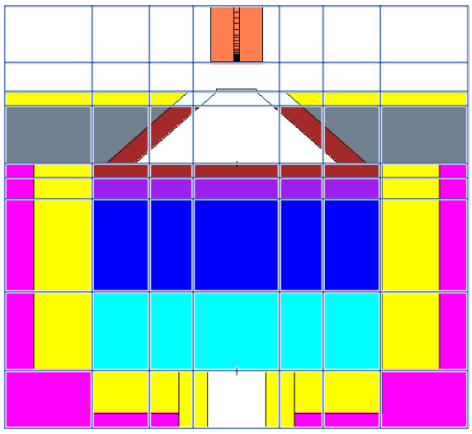

Fig. 4. Mesh 1- weight window mesh boundaries matching mostly with material boundaries for WWG.

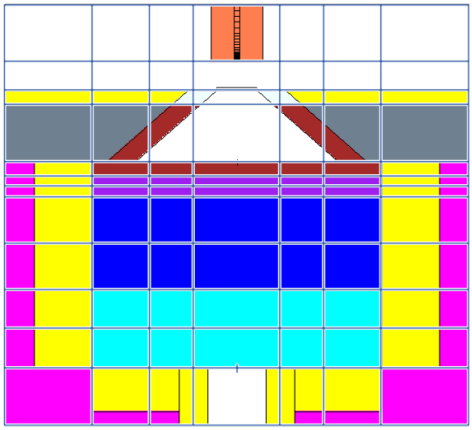

Fig. 5. Mesh 2 - finer mesh partitioning for WWG.

Table IV. Mesh Partitioning Used in Stage 1 Weight Window Generation

	Weight Window Mesh Partitioning	No. of Particle History Used in Stage 1
Case 3c	Mesh 1	2×10^8
Case 4a	Mesh 2	2×10^8

III. RESULTS AND DISCUSSION

1. Effect of Energy Structure of Mesh-Based Weight Window on overall performance

Table V compares the results of different choices of energy group structure for weight window generation on the overall performance of phantom-dose calculation. In stage 1, the number of particle history used was 4×10^8, the resulting relative error $R_{\bar{x}}$ of energy deposition at problem bin (at 11cm depth) was ~4%. In stage 2 calculation, the number of particle used was also 4×10^8. Case 1, a case without using weight window technique was included for comparison. Total CPU time of stage 1 and 2 was used to compute the FOM. Regardless of the choice of energy structure for weight window generation, the improvement of FOM was apparent.

For tally bin at 11 cm depth, the relative error $R_{\bar{x}}$ of total neutron dose rate of Case 2a and 2b (Method 1: equal lethargy energy group structure) were better than Case 2c and 2d (method 2: equal source population energy group structure). It is as small as 1.17%. On the other hand, computing time saving in stage 2 is more apparent when using method 2. For case 2e (method 3: hybrid method I) $R_{\bar{x}}$ of total neutron dose rate at 11 cm tally bin and computing time lie in between the above two methods. However, more tailored hybrid method I (Case2f) can reach as small $R_{\bar{x}}$ as method 1. For Case 2g (method 4, hybrid method II), $R_{\bar{x}}$ of total neutron dose rate of tally bin at 11 cm is 1.47%, slightly larger than Case 2f. The CPU time is slightly less than Case 2f. The best FOM calculated based on $R_{\bar{x}}$ of total neutron dose rate of tally bin at 11 cm depth is ~0.9 (Case 2f and Case 2a), ~300 times better than the case without using weight window technique (Case 1).

The RBE dose distribution in the phantom along the centerline is shown in Fig. 6. The photon dose comes mainly from the (n,γ) reaction of thermal neutrons with hydrogen in the brain phantom. Fig. 7 shows the $R_{\bar{x}}$ of total neutron dose rate of each bin along the centerline in the phantom. For depth <12 cm. Case 2a of method 1 is the best case of all. The $R_{\bar{x}}$ are all < 1.2%. The average $R_{\bar{x}}$ is 0.95% as shown in Table V. The FOM calculated based on the average $R_{\bar{x}}$ is 1.4, ~60 time better than the case without using weight window technique. Table V also shows the apparent reduction of the average $R_{\bar{x}}$ of photon dose along the centerline by a factor of ~7 when weight window technique is applied. Compared to neutron dose rate, $R_{\bar{x}}$ of photon dose rate is less sensitive to the energy group structure used for weight window generation.

Since Case 2a of method 1 provides the best FOM based on $R_{\bar{x}}$ of total neutron dose rate along the centerline in the phantom (for depth <12 cm), and less effort is required to generate the equal lethargy energy group structure, it is recommended to be used for WWG for this problem.

Table V. Effect of Energy Group Structure for Weight Window Generation on the Overall Performance of Weight Window Technique

	Case 1	Case 2a	Case 2b	Case 2c	Case 2d	Case 2e	Case 2f	Case 2g
Stage 1: Weight window generation (NPS = 4×10^8, $R_{\bar{x}}$ of energy deposition at problem bin = 4.17%)								
CPU time (min)	-	4720.1	4756.3	4744.9	4754.9	4727.7	4751.8	4737.7
Stage 2: In-phantom dose calculation (NPS = 4×10^8)								
CPU time (min)	4136.2	3176.0	2820.5	2027.1	1891.0	2567.7	3024.4	2963.8
$R_{\bar{x}}$ of total neutron dose rate of tally bin (at 11cm depth)	27.29%	1.17%	1.25%	2.27%	1.77%	1.54%	1.15%	1.47%
Average $R_{\bar{x}}$ of total neutron dose rate [a]	10.13%	0.95%	1.06%	1.58%	1.64%	1.28%	1.01%	1.19%
Maximum $R_{\bar{x}}$ of total neutron dose rate [a]	27.29%	1.20%	1.45%	2.27%	1.97%	2.14%	1.65%	1.82%
Average $R_{\bar{x}}$ of photon dose rate [a]	3.94%	0.56%	0.52%	0.66%	0.55%	0.51%	0.61%	0.45%
Average $R_{\bar{x}}$ of total dose rate [a]	4.90%	0.55%	0.58%	0.84%	0.85%	0.69%	0.59%	0.64%
Total: stage 1 + stage 2								
Total CPU time (min)	4136.2	7896.1	7576.8	6772.0	6645.9	7295.4	7776.1	7701.5
Total CPU time ratio (relative to Case 1)	-	1.91	1.83	1.64	1.61	1.76	1.88	1.86
FOM based on $R_{\bar{x}}$ of total neutron dose of tally bin (at 11cm)	0.003	0.925	0.845	0.287	0.480	0.578	0.972	0.601
FOM based on average $R_{\bar{x}}$ of total neutron dose rate [a]	0.024	1.403	1.175	0.592	0.559	0.837	1.261	0.917
FOM based on maximum $R_{\bar{x}}$ of total neutron dose rate [a]	0.003	0.879	0.628	0.287	0.388	0.299	0.472	0.392
FOM based on average $R_{\bar{x}}$ of photon dose rate [a]	0.156	4.038	4.881	3.390	4.974	5.270	3.456	6.412
FOM based on average $R_{\bar{x}}$ of total dose rate [a]	0.101	4.187	3.923	2.093	2.083	2.879	3.694	3.170

[a] Along the centerline up to 12cm depth

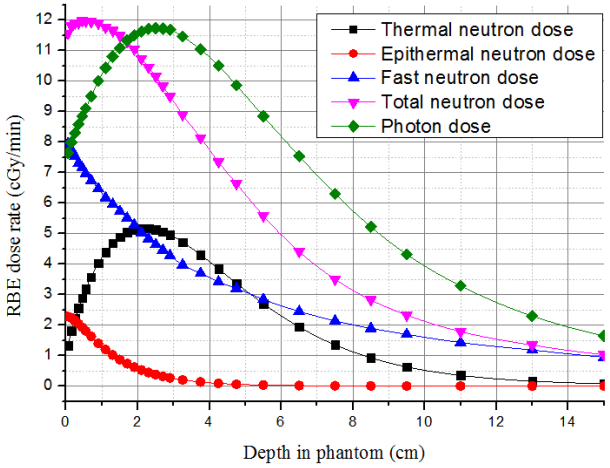

Fig. 6. In-phantom dose distribution along the centerline.

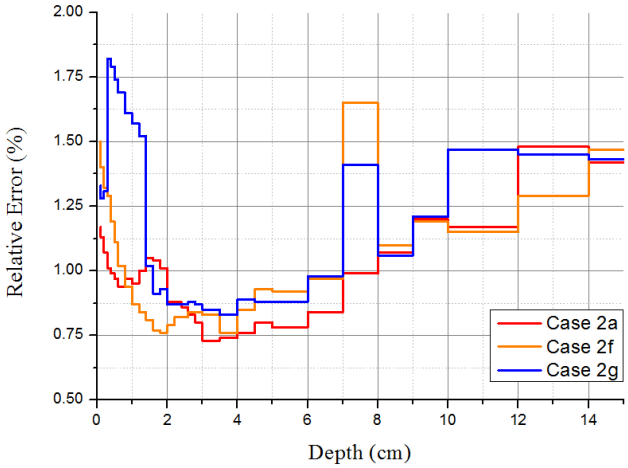

Fig. 7. Relative error of total neutron dose rate along the centerline in the phantom.

2. Effect of Number of Particle History Used for Stage 1 Mesh-Based Weight Window Generation

Table VI compares the effect of number of particle history (NPS) used in Stage 1 weight window generation on the overall performance of the calculation. Reference case is Case 2a in which NPS of stage 1 is 4×10^8 particles. The CPU time spent in stage 1 is 4720 minutes. $R_{\bar{x}}$ of the energy deposition at the problem bin is 4.2%. Using this weight window for stage 2 calculation, the average $R_{\bar{x}}$ of the total neutron dose rate at the tally bin along the centerline can be reduced to ~1%. The CPU time is ~3200 min. FOM is 1.4.

If the NPS used in stage 1 is reduced to 4×10^7 (Case 3a), $R_{\bar{x}}$ of problem bin of stage 1 increases to ~12%. Both the CPU time and $R_{\bar{x}}$ of neutron dose rate of tally bin in stage 2 increase. The FOM becomes very poor, ~0.052.

NPS of 2×10^8 particles (Case 3c) seems to be a proper choice for stage 1 weight window generation. The $R_{\bar{x}}$ at the problem bin is ~6%. At stage 2, the average $R_{\bar{x}}$ of total neutron dose rate is 1.2%, slightly larger than Case 2a. The total CPU time is 32% less than Case 2a and the FOM is close to Case 2a. This result implies that during the stage 1 weight window generation, the NPS that can provide $R_{\bar{x}}$ at the problem bin ~6% may be good enough.

3. Effect of Spatial Partitioning for Mesh-Based Weight Window Generation

Table VII shows that using finer meshes (Mesh 2) than Mesh 1 for weight window generation results in more computing time in stage 2 without improving the precision. The FOM becomes worse.

Table VI. Effect of Number of Particle History Used for Weight Window Generation on the Overall Performance of Weight Window Technique

	Case 2a	Case 3a	Case 3b	Case 3c
Stage 1: Weight window generation				
Number of particle history	4×10^8	4×10^7	1×10^8	2×10^8
CPU time (min)	4720.1	471.3	1183.7	2319.0
$R_{\bar{x}}$ of energy deposition at problem bin (at 11cm depth)	4.17%	12.13%	8.18%	5.88%
Stage 2: In-phantom dose calculation (NPS=4×10^8)				
CPU time (min)	3176.0	9460.5	5496.7	3045.2
$R_{\bar{x},2}$ of total dose rate at tally bin (at 11cm depth)	1.17%	9.18%	1.50%	1.22%
Average $R_{\bar{x}}$ of total neutron dose rate [a]	0.95%	4.39%	1.25%	1.18%
Average $R_{\bar{x}}$ of photon dose rate [a]	0.56%	0.53%	1.35%	0.53%
Total (stage 1 + stage 2)				
Total CPU time (min)	7896.1	9931.8	6680.4	5364.3
Total CPU time ratio (relative to Case 1)	1.91	2.40	1.62	1.30
FOM based on average $R_{\bar{x}}$ of total neutron dose rate [a]	1.403	0.052	0.958	1.339
FOM based on average $R_{\bar{x}}$ of photon dose rate [a]	4.038	3.584	0.821	6.637

[a] Along the centerline up to 12cm depth

Table VII. Effect of Mesh Partitioning for Weight Window Generation on the Overall Performance of Weight Window Technique

	Case 3c	Case 4a
Mesh Partitioning	Mesh 1	Mesh 2
Stage 1: Weight window generation (NPS=2×10^8)		
CPU time (min)	2319.0	2385.8
$R_{\bar{x}}$ of energy deposition at problem bin (at 11cm depth)	5.88%	5.88%
Stage 2: In-phantom dose calculation (NPS=4×10^8)		
CPU time (min)	3045.2	5097.5
$R_{\bar{x},2}$ of total neutron dose rate at tally bin (at 11cm depth)	1.22%	1.47%
Average $R_{\bar{x}}$ of total neutron dose rate [a]	1.18%	1.10%
Average $R_{\bar{x}}$ of photon dose rate [a]	0.53%	0.50%
Total(stage 1 + stage 2)		
Total CPU time (min)	5364.3	7483.3
Total CPU time ratio (relative to Case 1)	1.30	1.81
FOM based on average $R_{\bar{x}}$ of total neutron dose rate [a]	1.339	1.104
FOM based on average $R_{\bar{x}}$ of photon dose rate [a]	6.637	5.345

[a] Along the centerline up to 12cm depth

IV. CONCLUSIONS

Result of this study shows that properly applying the weight window technique in MCNPX calculation can effectively reduce the statistical errors of the in-phantom dose rate with only ~30% increasing in total computing time.

Suggestions for weight window generation includes: (1)aligning mesh boundaries with material boundaries, (2) using equal lethargy or properly combined with equal neutron source population for energy group structure, and (3) using number of particles that results in $R_{\bar{x}}$ <6% at the problem bin.

After using this weight window technique in MCNP calculation, the in-phantom dose rate at depth < 12 cm can be obtained with statistical error ~1% within 2hrs using 48 threads of our PC-cluster.

Deterministic code such as ADVANTG [6] using CADIS method for weight window generation for MCNP calculation is worthwhile to explore in future study.

REFERENCES

1. D. B. Pelowitz, "MCNPX User's Manual, Version 2.6.0," Report LA-CP-07-1473 (2008).
2. ICRU Report 46, "Photon, Electron, Proton and Neutron Interaction Data for Body Tissue," International Commission on Radiation Units and Measurement (1992).
3. R.S. Caswell, J. J. Coyne, M. L. Randolph, "*KERAM Factors of Elements and Compounds for Neutron Energies Below 30MeV*," Int. J Appl. Radiat. Isot., 33:1227 (1982).
4. IAEA-TECDOC-1223, "Current Status of Neutron Capture Therapy", International Atomic Energy Agency (2001).
5. A. Haghighat, *Monte Carlo Methods for Particle Transport*, P.102, CRC Press (2014).
6. S. W. Mosher, A. M. Bevill, S. R. Johnson, A. M. Ibrahim, C. R. Daily, T. M. Evans, J. C. Wagner, J. O. Johnson, R. E. Grove, "ADVANTG-An Automated Variance Reduction Parameter Generator," Oak Ridge National Laboratory, Report ORNL/TM-2013/416 (2013).

AKNOWLEDGEMENT

This work is supported by Industrial Technology Research Institute, Republic of China.